

Efficient Photodimerization Reaction of Anthracene in Supercritical Carbon Dioxide

Christopher E. Bunker,[†] Harry W. Rollins,[†] James R. Gord,[‡] Ya-Ping Sun^{†,*}

Department of Chemistry, Howard L. Hunter Chemistry Laboratory, Clemson University, Clemson, South Carolina 29634-1905, and Wright Laboratory, Aero Propulsion and Power Directorate, Wright–Patterson Air Force Base, Ohio 45433-7103

Received May 20, 1997

The photodimerization reaction of anthracene in supercritical CO₂ was studied systematically at different CO₂ densities. Unlike in normal liquid solvents, the reaction in supercritical CO₂ is significant even at anthracene concentrations as low as a few micromolar. At comparable anthracene concentrations, the photodimerization reaction is 1 order of magnitude more efficient in CO₂ than in normal liquid solvents. The dramatic increases in the photodimerization reaction efficiency in supercritical CO₂ may be explained by a mechanism in which the reaction is diffusion-controlled even when the diffusion rate constants are on the order of 10¹¹ M⁻¹ s⁻¹. The results also show that the efficient photodimerization reaction of anthracene is hardly affected by the local density augmentation (or solute–solvent clustering) in supercritical CO₂.

Introduction

Supercritical fluids are widely investigated as alternatives to normal liquid solvents for a variety of physical and chemical processes.^{1,2} Particularly, supercritical CO₂ has attracted much attention, due largely to the ambient critical temperature and the environmentally benign characteristics of the fluid. For example, supercritical CO₂ has been used in the preparation and processing of perfluorinated polymers.³ Since supercritical CO₂ is inert to free radicals, radical-initiated polymerization reactions can be carried out in supercritical CO₂ with results similar to or better than those in organic solvents.⁴ Supercritical CO₂–surfactant systems have also been examined for the handling of biological materials.⁵

For the use of supercritical fluids as media for chemical reactions, effects of the unique properties of supercritical fluids on reaction rates, selectivity, and product distributions need to be understood. There have been several reports of experimental investigations of chemical reactions in supercritical fluids. Weedon and co-workers studied a photofries rearrangement reaction of naphthyl acetate in supercritical CO₂.⁶ The product yield ratios of photofries to hydrogen abstraction were found to increase significantly in the near-critical density region. The increase was attributed to solute–solvent interactions that effectively cage the radical species allowing a more efficient recombination.⁶ Dimerization reactions have also been studied in supercritical fluids.^{7,8} Fox, Johnston, and co-workers reported an investigation of the

photodimerization reaction of isophorone in ambient supercritical fluids CO₂ and trifluoromethane.⁷ It was concluded on the basis of a detailed study of the stereo- and regioselective product yields that the photodimerization reaction is dependent on both solvent polarity and solvent reorganization. Kimura *et al.* investigated solvent density effects on the dimerization reaction of 2-methyl-2-nitrosopropane in supercritical CO₂, chlorotrifluoromethane, and trifluoromethane.⁸ The results show three distinct density regions in which the reaction is controlled by different combinations of energetic effects and packing effects. Diels–Alder reactions have been studied systematically in supercritical fluids.^{9–15} Effects of supercritical solvent environment on the reaction kinetics have been examined. Tester and co-workers reported a correlation of experimental data and kinetic models for the Diels–Alder reaction of cyclopentadiene and ethyl acrylate in supercritical CO₂.¹⁰ The results suggest that the reaction in the supercritical solvent environment is subject to significant local density (or solute–solvent clustering)^{16,17} effects. For the Diels–Alder reaction of cyclopentadiene and *p*-benzoquinone, Isaacs and Keating observed a 20% or so rate increase from liquid diethyl ether to supercritical CO₂ as the solvent.¹¹ However, significant rate increases for bimolecular reactions in supercritical fluids have been anticipated with the consideration that the densities of a supercritical fluid are much lower than those of normal

(8) (a) Kimura, Y.; Yoshimura, Y.; Nakahara, M. *J. Chem. Phys.* **1989**, *90*, 5679. (b) Kimura, Y.; Yoshimura, Y. *J. Chem. Phys.* **1992**, *96*, 3085.

(9) (a) Oppolzer, W. *Comprehensive Organic Synthesis*, Pergamon Press: Oxford, 1991; Vol. 5, pp 315–400. (b) Carruthers, W. *Cycloaddition Reactions in Organic Synthesis*, Pergamon Press: Oxford, 1990.

(10) Weinstein, R. D.; Renslo, A. R.; Danheiser, R. L.; Harris, J. G.; Tester, J. W. *J. Phys. Chem.* **1996**, *100*, 12337.

(11) Isaacs, N. S.; Keating, N. *J. Chem. Soc., Chem. Commun.* **1992**, 876.

(12) Paulaitis, M. E.; Alexander, G. C. *Pure Appl. Chem.* **1987**, *59*, 61.

(13) Kim, S.; Johnston, K. P. *Chem. Eng. Commun.* **1988**, *63*, 49.

(14) (a) Ikushima, Y.; Ito, S.; Asano, T.; Yokoyama, T.; Saito, N.; Hatakeda, K.; Goto, T. *J. Chem. Eng. Jpn.* **1990**, *23*, 96. (b) Ikushima, Y.; Saito, N.; Arai, M. *Bull. Chem. Soc. Jpn.* **1991**, *64*, 282. (c) Ikushima, Y.; Saito, N.; Arai, M. *J. Phys. Chem.* **1992**, *96*, 2293.

(15) Rhodes, T. A.; O'Shea, K.; Bennett, G.; Johnston, K. P.; Fox, M. A. *J. Phys. Chem.* **1995**, *99*, 9903.

(16) Kim, S.; Johnston, K. P. *Ind. Eng. Chem. Res.* **1987**, *26*, 1206.

(17) Eckert, C. A.; Knutson, B. L. *Fluid Phase Equil.* **1993**, *83*, 93.

[†] Clemson University.

[‡] Wright–Patterson Air Force Base.

* Abstract published in *Advance ACS Abstracts*, October 1, 1997.

(1) For recent reviews, see: (a) Savage, P. E.; Gopalan, S.; Mizan, T. I.; Martino, C. J.; Brock, E. E. *AIChE J.* **1995**, *41*, 1723. (b) Clifford, T.; Bartle, K. *Chem. Ind.* **1996**, 449.

(2) Shaw, R. W.; Brill, T. B.; Clifford, A. A.; Eckert, C. A.; Franck, E. U. *Chem. Eng. News* **1991**, Dec. 23, 26.

(3) DeSimone, J. M.; Maury, E. E.; Menciloglu, Y. Z.; McClain, J. B.; Romack, T. J.; Combes, J. R. *Science* **1994**, *265*, 356.

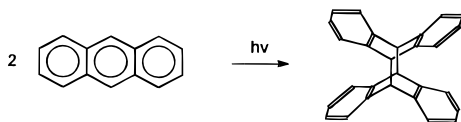
(4) Rollins, H. W.; Sun, Y.-P. Manuscript in preparation.

(5) Johnston, K. P.; Harrison, K. L.; Clarke, M. J.; Howdle, S. M.; Heitz, M. P.; Bright, F. V.; Carlier, C.; Randolph, T. W. *Science* **1996**, *271*, 624.

(6) Andrew, D.; Des Islet, B. T.; Margaritis, A.; Weedon, A. C. *J. Am. Chem. Soc.* **1995**, *117*, 6132.

(7) Hrnjez, B. J.; Mehta, A. J.; Fox, M. A.; Johnston, K. P. *J. Am. Chem. Soc.* **1989**, *111*, 2662.

liquid solvents and, as a result, molecular diffusivities in supercritical fluids are much higher. In addition, the densities of a supercritical fluid are easily tunable with changes in pressure under isothermal conditions, which thus allows studies of chemical reactions in a tunable solvent environment from gaslike to liquidlike. In this paper we report a systematic study of the photodimerization reaction of anthracene in supercritical CO₂ to demonstrate that the rate of a bimolecular reaction in supercritical CO₂ may be enhanced by 1 order of magnitude in comparison with the rates in normal liquid solvents such as benzene.



Unlike in normal liquid solvents,^{18–22} the photodimerization reaction of anthracene in supercritical CO₂ is significant even at anthracene concentrations as low as a few micromolar. The dramatic increases in the photodimerization reaction efficiency in supercritical CO₂ may be explained by a mechanism in which the reaction is diffusion-controlled even when the diffusion rate constants are on the order of 10¹¹ M⁻¹ s⁻¹. The results also show that the efficient photodimerization reaction of anthracene is hardly affected by the local density augmentation (or solute–solvent clustering) in supercritical CO₂.

Experimental Section

Materials. Anthracene (99%) was obtained from Aldrich and used without further purification. Hexane (spectrophotometry grade) was obtained from Burdick & Jackson, and benzene (99+%) was obtained from Aldrich. CO₂ (99.9999%) was obtained from Air Products and used without further purification.

Measurements. Photoirradiation was carried out by use of a photochemistry setup consisting of an optical bench and a 450 W xenon arc lamp obtained from Spectral Energy. A water filter was used for the absorption of infrared radiation. Excitation wavelengths for photoirradiation were selected by using a Spex 1681 monochromator with a large slit of 19 nm band pass (for excitation at 375 nm) or by using color glass sharp cut (330 nm) and band pass (367 nm) filters.

Photodimerization reactions of anthracene in supercritical CO₂ were carried out by using a high-pressure setup. The system pressure was generated by a Teflon-packed syringe pump obtained from the High Pressure Equipment Co. and monitored by a precision pressure gauge (Heise-901A) obtained from Dresser Industries. The calibrated accuracy of the pressure gauge is better than ±1 psia at 1100 psia. The system temperature was controlled and monitored by an RTD temperature controller (Omega 4200A) coupled with a pair of cartridge heaters (Gauger 150W) inserted into the optical cell body. Two high-pressure optical cells with the same design but different optical path lengths were used. Both cells are cylindrical with two quartz windows (2.5 cm in diameter and 0.95 cm in thickness) at the two ends of the cell. The optical path lengths of the two cells are 2.2 and 8.0 cm with calibrated cell volumes of 5.3 and 19.5 mL, respectively.

UV/vis absorption spectra were recorded on a computer-controlled Shimadzu UVPC-2101 spectrophotometer. Fluorescence spectra were obtained on a Spex Fluorolog-2 photon-counting emission spectrometer equipped with a 450 W xenon source and a Hamamatsu R928 photomultiplier tube. Fluorescence measurements in supercritical CO₂ were carried out by use of a cube-shaped high-pressure optical cell made from stainless steel. The cell chamber (calibrated volume 1.87 mL) consists of four channels which open at the four side walls of the cell. Three of the channels are for accommodating optical windows, and the fourth one is for cell cleaning. The three quartz windows (12.7 mm in diameter and 5 mm in thickness) are sealed using Teflon O-rings. The optical paths of the cell for absorption (180°) and fluorescence (90°) measurements are 30.5 and 7.5 mm, respectively. All fluorescence spectra were corrected for nonlinear instrumental response of the emission spectrometer using predetermined correction factors.

For the determination of fluorescence and photodimerization quantum yields, specially designed optical cell holders were used to ensure the reproducibility of the cell geometry with respect to the excitation and emission light paths.

Fluorescence decays were measured using a time-correlated single-photon-counting apparatus. The excitation source was a Spectra-Physics 3690 Tsunami mode-locked Ti:sapphire laser configured to produce an ~82 MHz train of pulses at 740 nm with a nominal pulse width of ≤2 ps. The repetition rate of the pulse train was reduced to 4 MHz using a Spectra-Physics 3980 pulse selector. The laser output was frequency-doubled. The detector consists of a Hamamatsu R3809U-01 micro-channel plate photomultiplier (MCP) tube in a Hamamatsu C2773 thermoelectrically cooled housing. The MCP tube was biased at -3000 V using a Stanford Research Systems PS350 power supply. The detector electronics include two EG&G Ortec 9307 discriminators, a Tennelec TC-864 time-to-amplitude converter/biased amplifier, and a Tennelec PCA-Multiport-E multichannel analyzer. The time resolution of the setup as measured by the half-width of the instrument response function was ~60 ps. Fluorescence decays were monitored at 410 nm through an American Holographic DB-10S double-subtractive monochromator. Fluorescence lifetimes were determined from observed decay curves and instrument response functions by use of the Marquardt nonlinear least-squares method.²³

In the preparation of anthracene solutions in supercritical CO₂, a hexane solution of anthracene was added to the high-pressure optical cell. The cell was purged with a slow stream of nitrogen gas to remove the solvent hexane. A procedure of repeatedly filling and discharging with low-pressure CO₂ gas (<100 psia) was used to eliminate trace amounts of oxygen trapped in the optical cell chamber. The cell was then sealed and thermostated at the desired temperature before CO₂ was introduced. Actual anthracene concentrations were determined based on absorption spectral measurements.

Experimental viscosity values of supercritical CO₂ are available at selected temperatures and pressures.²⁴ Interpolation for obtaining the values under our experimental conditions was made using the empirical equation due to Jossi, Stiel, and Thodos:²⁵

$$[(\eta - \eta^0)\xi_T + 1]^{1/4} = a_0 + a_1\rho_r + a_2\rho_r^2 + a_3\rho_r^3 + a_4\rho_r \quad (1)$$

$$\xi_T = (T_c/M^3 P_c^4)^{1/6} \quad (2)$$

where η and η^0 are viscosities of the fluid and low-pressure gas, respectively, P_c and T_c are the critical parameters, M denotes molecular weight, and ρ_r represents reduced density. The parameters a_i in eq 1 generalized for nonpolar fluids are available in the literature.²⁵ However, in order to be more

(18) (a) Bowen, E. J. *Adv. Photochem.* **1963**, *1*, 23. (b) Stevens, B. *Adv. Photochem.* **1971**, *8*, 161.

(19) Becker, H.-D. *Chem. Rev.* **1993**, *93*, 145.

(20) Bouas-Laurent, H.; Castellán, A.; Desvergne, J.-P. *Pure Appl. Chem.* **1980**, *52*, 2633.

(21) Saltiel, J.; Atwater, B. W. *Adv. Photochem.* **1988**, *14*, 1.

(22) Bouas-Laurent, H.; Desvergne, J.-P. In *Photochromism, Molecules and Systems*; Dürr, H., Bouas-Laurent, H., Eds.; Elsevier: Amsterdam, 1990; p 561.

(23) O'Connor, D. V.; Phillips, D. *Time-Correlated Single Photon Counting*; Academic Press: New York, 1984.

(24) Stephan, K.; Lucas, K. *Viscosity of Dense Fluids*; Plenum Press: New York, 1979.

(25) (a) Jossi, J. A.; Stiel, L. I.; Thodos, G. *AIChE J.* **1962**, *8*, 59. (b) Reid, R. C.; Prausnitz, J. M.; Poling, B. E. *The Properties of Gases and Liquids*; McGraw-Hill: New York, 1987.

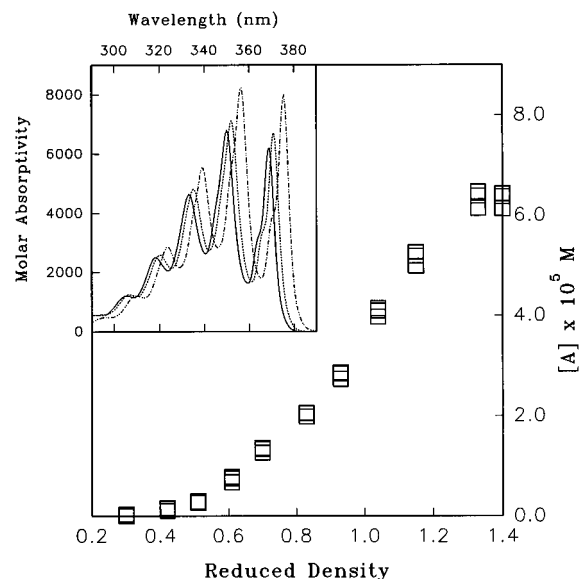


Figure 1. Solubilities of anthracene in supercritical CO₂ at 35 °C as a function of CO₂ reduced density. Inset: Absorption spectra of anthracene in CO₂ at reduced densities of 1.0 (—) and 1.9 (···) and in room-temperature hexane (---).

accurate specifically for CO₂ under our experimental conditions, the parameters were obtained from the experimental viscosity data through a least-squares regression. For CO₂ in the temperature range of 35–57 °C and pressures up to 400 bar, the parameters are $a_0 = 0.9975$, $a_1 = 0.2061$, $a_2 = 0.6998$, $a_3 = -0.5258$, and $a_4 = 0.1372$.

Results

Solubilities of Anthracene in CO₂. Solubilities of anthracene in supercritical CO₂ were determined as a function of density by use of the UV absorption method. The UV absorption spectra of anthracene in CO₂ at low and high densities are compared with the spectrum in room-temperature hexane in Figure 1. The molar absorptivity at the absorption band maximum ϵ_{MAX} for anthracene in hexane is 8200 M⁻¹ cm⁻¹, which agrees well with the literature results. In the determination of molar absorptivities of anthracene in supercritical CO₂ at 35 °C at different densities, a dilute anthracene solution of 2.5×10^{-5} M was used. The ϵ_{MAX} values in CO₂ are somewhat smaller than that in room-temperature hexane (Figure 1). They are also slightly density dependent, with $\epsilon_{\text{MAX}} = 7100$ M⁻¹ cm⁻¹ at the CO₂ reduced density of 1.9. Shown in Figure 2 are the observed molar absorptivities of the first three absorption peaks as a function of CO₂ reduced density.

With the known molar absorptivities of anthracene, the solubilities in supercritical CO₂ at different reduced densities were determined spectrophotometrically in terms of Lambert–Beer's law. In the measurements, a known amount of anthracene that corresponds to a concentration of 6.4×10^{-5} M was added to a high-pressure optical cell. Absorption spectra were carefully recorded at different CO₂ reduced densities from 0.3 to 1.4. At each CO₂ reduced density, the supercritical solution was vigorously stirred and allowed to equilibrate for ~15 min prior to absorption spectral measurements. Shown in Figure 1 is a plot of saturated anthracene concentration vs CO₂ reduced density at 35 °C. Apparently, the amount of anthracene added to the optical cell becomes completely dissolved at the CO₂ reduced densi-

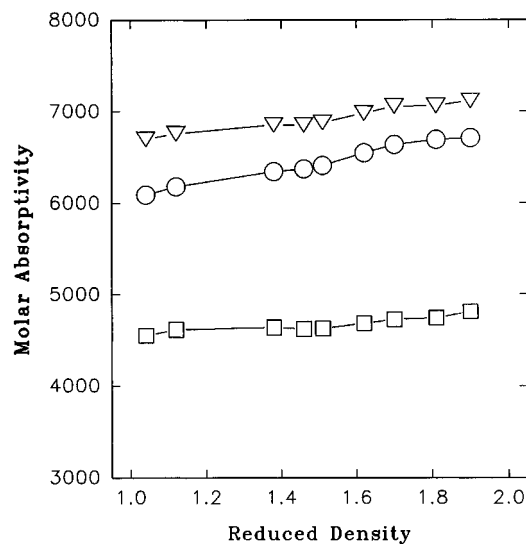


Figure 2. Molar absorptivities of anthracene in supercritical CO₂ at 35 °C as a function of CO₂ reduced density: (○) first peak, (▽) second peak, and (□) third peak.

ties of 1.3 and higher. According to Figure 1, an anthracene concentration of 2.5×10^{-5} M in supercritical CO₂ at 35 °C can be obtained at reduced densities of ~0.9 and higher.

Photodimerization. Photodimerization reactions of anthracene were carried out in supercritical CO₂ at 35 °C. In the preparation of a supercritical solution for photoirradiation, a high-pressure optical cell with an 8 cm optical path length was loaded with ~1 mL of an anthracene solution in hexane with known concentration. The solvent hexane was removed by purging with a slow stream of nitrogen gas. The optical cell was also purged to remove trace amounts of oxygen trapped in the cell chamber by repeatedly filling and releasing low-pressure CO₂ gas. The cell was then sealed and thermostated at the desired temperature before supercritical CO₂ was introduced. Since the volume and optical path length of the high-pressure cell were calibrated, the anthracene concentration in supercritical CO₂ was determined spectrophotometrically. The anthracene concentrations used in photodimerization reactions were kept below the anthracene solubility limits at the employed CO₂ reduced densities. The reaction progress was monitored spectrophotometrically by following the disappearance of anthracene monomer. Absorption spectra of the anthracene solution in supercritical CO₂ under photoirradiation were measured at different time intervals. Shown in Figure 3 are results from the photoirradiation of an anthracene solution of 3.8×10^{-5} M in supercritical CO₂ at 35 °C and the reduced density of 1.9. The systematic decrease in absorbance with increasing photoirradiation time is attributed to the conversion of anthracene monomers to anthracene dimers, which absorb at much shorter wavelengths (<300 nm).²⁶ A plot of observed absorbances at 320 nm as a function of photoirradiation time is also shown in Figure 3 for low monomer to dimer conversions of less than <25%. The plot is essentially linear, so that $dA(\lambda)/dt$ is a constant in the low-conversion region. The anthracene photodimerization quantum yield Φ_{DIM} can be related to the rate of anthracene monomer disappear-

(26) Birks, J. B.; Appleyard, J. H.; Pope, R. *Photochem. Photobiol.* **1963**, *2*, 493.

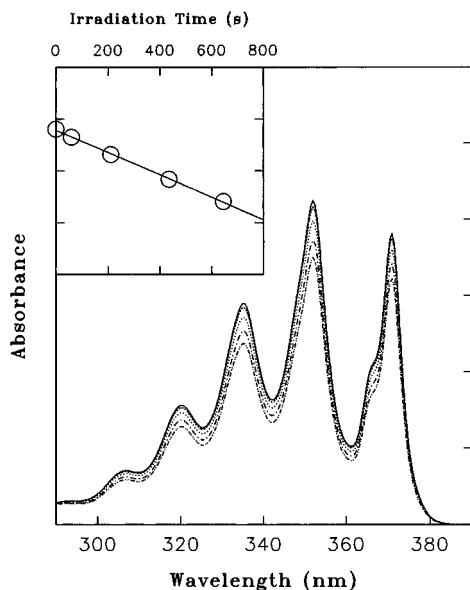


Figure 3. Absorption spectra of anthracene in CO₂ ([A] = 3.8 × 10⁻⁵ M, 35 °C, and reduced density of 1.9) obtained at different time intervals of photoirradiation. Inset: Dependence of observed absorbance on irradiation time for the low-monomer-to-dimer-conversion region of <25%.

ance:²⁷

$$2\Phi_{\text{DIM}} = -(\text{d}[A]/\text{d}t)/I_{\text{ABS}} = -[\text{d}A(\lambda)/\text{d}t]/\epsilon(\lambda)I_{\text{ABS}} \quad (3)$$

where I_{ABS} is the intensity of absorbed light, $\epsilon(\lambda)$ is the molar absorptivity of anthracene at wavelength λ , and l is the absorption path length. In the determination of Φ_{DIM} values for anthracene in supercritical CO₂, I_{ABS} was obtained by use of the photodimerization yield of anthracene in room-temperature benzene as a reference.^{28,29} In the photochemical experiment, benzene solutions of anthracene were irradiated under the same conditions as those for the solutions of anthracene in supercritical CO₂. The rate of anthracene monomer disappearance $-\text{d}[A]/\text{d}t$ in room-temperature benzene is also constant at low conversions of less than 25%. Thus,

$$\Phi_{\text{DIM,CO}_2} = \Phi_{\text{DIM,BEN}}(\text{d}[A]/\text{d}t)_{\text{CO}_2}/(\text{d}[A]/\text{d}t)_{\text{BEN}} \quad (4)$$

where $\Phi_{\text{DIM,BEN}}$ is the photodimerization yield of anthracene in an air-saturated benzene solution at room temperature. For the anthracene concentrations of 3.28 × 10⁻⁴ and 5.74 × 10⁻³ M, $\Phi_{\text{DIM,BEN}}$ values can be obtained through interpolations from the results reported in the literature.^{28,29} The results from the two references are very similar. The photodimerization yields thus obtained for anthracene in supercritical CO₂ at 35 °C and the reduced density of 1.9 are 7.2 × 10⁻⁴ and 1.6 × 10⁻² for the anthracene concentrations of 2.3 × 10⁻⁵ and 2.5 × 10⁻⁴ M, respectively. As expected, the yields increase with increasing anthracene concentrations.

Photodimerization yields of anthracene at a fixed concentration were also determined in CO₂ at different reduced densities at 35 °C. Since the result at the lowest CO₂ density considered ($\rho_r = 1.0$) is particularly impor-

Table 1. Photodimerization Yields and Fluorescence Lifetimes of Anthracene (2.5 × 10⁻⁵ M) in Supercritical CO₂ at 35 °C as a Function of Reduced Density

| ρ_r | η (cP) | $\Phi_{\text{DIM}} \times 10^{-3}$ | τ_F (ns) ^a |
|----------|-------------|------------------------------------|----------------------------|
| 1.0 | 0.034 | 1.9 ^b | 7.81 |
| 1.13 | 0.039 | 1.6 | 7.73 |
| 1.16 | 0.040 | 1.6 | 7.71 |
| 1.19 | 0.042 | 1.7 | 7.70 |
| 1.25 | 0.044 | 1.5 | 7.66 |
| 1.30 | 0.047 | 1.5 | 7.63 |
| 1.40 | 0.052 | 1.2 | 7.57 |
| 1.45 | 0.055 | 1.4 | 7.55 |
| 1.58 | 0.063 | 1.1 | 7.48 |
| 1.71 | 0.074 | 1.1 | 7.41 |
| 1.74 | 0.077 | 1.0 | 7.39 |
| 1.81 | 0.087 | 0.90 | 7.36 |
| 1.91 | 0.097 | 0.75 | 7.31 |

^a Lifetime values at the listed reduced densities are determined by interpolation of the experimental data. ^b An average of five repeats with an estimated error margin of ±12%.

tant in mechanistic analysis, the measurements were repeated. As shown in Table 1 for the anthracene concentration of 2.5 × 10⁻⁵ M, the observed photodimerization yields gradually decrease with increasing CO₂ reduced densities.

Fluorescence. Fluorescence competes with photodimerization in the excited singlet state of anthracene. For anthracene in supercritical CO₂ at 35 °C, fluorescence parameters were determined at a series of reduced densities. The fluorescence quantum yields Φ_F were measured at CO₂ reduced densities from 0.8 to 1.9 on the basis of integrated fluorescence intensities. The observed Φ_F values are essentially CO₂ density independent, with an average yield of 0.3 using 9-cyanoanthracene ($\Phi_F = 1.0$)³⁰ as a standard.

Fluorescence decays of anthracene in supercritical CO₂ at 35 °C were measured on a time-correlated single-photon-counting setup. Measurements were carried out at a series of CO₂ reduced densities from 0.36 to 1.9. All of the observed decay curves can be deconvoluted well from instrumental response functions using a monoexponential equation. Shown in Figure 4 is an example of the fluorescence decay results. The fluorescence lifetimes thus obtained are also shown in Table 1. The results indicate that the fluorescence lifetimes of anthracene in supercritical CO₂ are slightly density dependent, becoming somewhat shorter at higher CO₂ densities (Table 1). The decrease in the fluorescence lifetime of anthracene with increasing CO₂ reduced density is due to the increase in the fluorescence radiative rate constant with increasing refractive index of the fluid³⁰ because the fluorescence quantum yield of anthracene remains essentially constant in the density region.

Great effort was made for the detection of possible anthracene excimer emissions in the supercritical solvent environment. Fluorescence spectra of saturated anthracene solutions in supercritical CO₂ at different reduced densities were recorded carefully. However, the results indicate no contributions from anthracene excimer emissions.³¹

Discussion

Photodimerization of anthracene is much more efficient in supercritical CO₂ than in normal liquid solvents such

(27) Yang, N. C.; Shold, D. M.; Kim, B. *J. Am. Chem. Soc.* **1976**, *98*, 6587.

(28) Saltiel, J.; Townsend, D. E.; Watson, B. D.; Shannon, P.; Finson, S. L. *J. Am. Chem. Soc.* **1977**, *99*, 884.

(29) Charlton, J. L.; Dabestani, R.; Saltiel, J. *J. Am. Chem. Soc.* **1983**, *105*, 3473.

(30) Hirayama, S.; Shobatake, K.; Tabayashi, K. *Chem. Phys. Lett.* **1985**, *121*, 228 and references cited therein.

(31) McVey, J. K.; Shold, D. M.; Yang, N. C. *J. Chem. Phys.* **1976**, *65*, 3375.

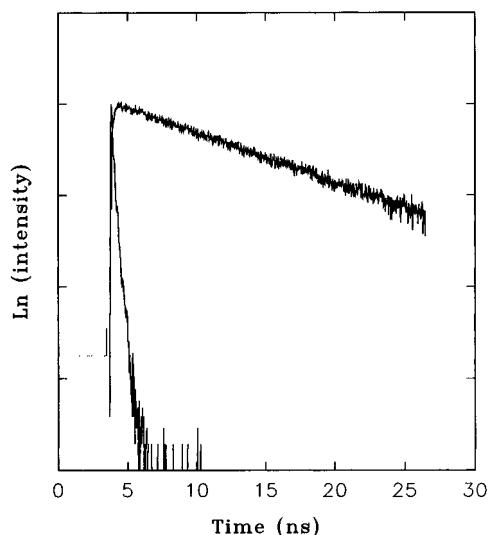


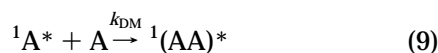
Figure 4. Fluorescence decay of anthracene in CO₂ (35 °C and reduced density of 0.96). The deconvolution from the instrument response function using a monoexponential equation yields τ_F of 7.85 ns ($\chi^2 = 1.04$).

as benzene. At comparable anthracene concentrations, photodimerization yields in supercritical CO₂ are 1 order of magnitude greater than those in normal liquid solvents.^{27–29,32,33} The results demonstrate that supercritical fluids may indeed be used to enhance chemical reaction efficiencies in addition to their advantages of being environmentally benign solvent systems. It is also very interesting that molecular diffusion still plays a critical role in the photodimerization of anthracene even when the diffusion rate constants are on the order of 10¹¹ M⁻¹ s⁻¹ in supercritical CO₂.

For the photodimerization of anthracene in normal liquid solvents, an excited singlet state mechanism has been established.²² The excited state processes of anthracene may be described as follows:



The involvement of an excimer intermediate has been suggested on the basis of the results in solutions and in 77 K solvent matrices.^{31,34–36} Thus, eq 8 may be rewritten as follows:²²



(32) Saltiel, J.; Dabestani, R.; Schanze, K. S.; Trojan, D.; Townsend, D. E.; Goedken, V. L. *J. Am. Chem. Soc.* **1986**, *108*, 2674.

(33) (a) Suzuki, M. *Bull. Chem. Soc. Jpn.* **1943**, *18*, 146. (b) Suzuki, M. *Bull. Chem. Soc. Jpn.* **1949**, *22*, 172. (c) Suzuki, M. *Bull. Chem. Soc. Jpn.* **1950**, *23*, 120.

(34) Cohen, M. D.; Ludmer, Z.; Yakhot, V. *Chem. Phys. Lett.* **1976**, *38*, 398.

(35) Chandross, E. A. *J. Chem. Phys.* **1965**, *43*, 4175.

(36) (a) Ferguson, J.; Mau, A. W. H. *Mol. Phys.* **1974**, *27*, 377. (b) Anderson, B. F.; Ferguson, J.; Morita, M.; Robertson, G. B. *J. Am. Chem. Soc.* **1979**, *101*, 1832.

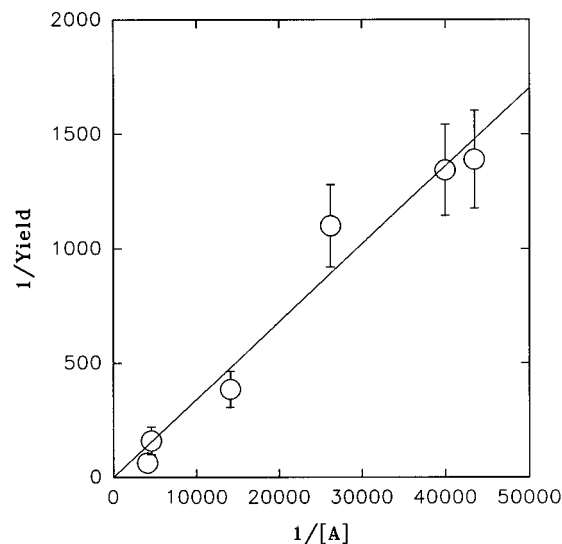


Figure 5. Plot of $1/\Phi_{DIM}$ vs $1/[A]$ for anthracene in supercritical CO₂ at 35 °C and reduced density of 1.9. The line (forced through the origin in the regression) has a slope of 0.034 M.



In the excited singlet state mechanism with an excimer intermediate, the observed anthracene photodimerization yield may be expressed as the product of the yield for excimer formation Φ_{DM} and the yield for dimer formation from the excimer intermediate Φ_{A_2} .

$$\Phi_{DIM} = \Phi_{DM}\Phi_{A_2} = \frac{k_{DM}[A]}{k_{DM}[A] + (1/\tau_F)} \Phi_{A_2} \quad (12)$$

where $\tau_F = 1/(k_F + k_{ISC} + k_{IM})$ is the fluorescence lifetime of anthracene in the absence of bimolecular processes and $\Phi_{A_2} = k_{DIM}/(k_{DIM} + k_{ID})$.

For anthracene photodimerization in normal liquid solvents, contributions from the excited triplet state of anthracene have been observed under certain experimental conditions.²⁹ The triplet state mechanism involves the formation of a doubly excited singlet state from the interaction of two excited triplet anthracene molecules. As a result, the triplet state contributions are dependent on the light intensity for photoirradiation. It has been shown²⁹ that a plot of $1/\Phi_{DIM}$ vs $1/[A]$ is linear in the absence of triplet state contributions but exhibits obvious downward curvatures when the triplet state contributions are significant at high light intensities for photoirradiation. For the photodimerization of anthracene in supercritical CO₂ under our experimental conditions, the triplet state contributions are likely small. Shown in Figure 5 is a plot of $1/\Phi_{DIM}$ vs $1/[A]$ for anthracene in CO₂ at 35 °C and the reduced density of 1.9, which exhibits no obvious downward curvature. Thus, in the further treatment of the experimental results of anthracene photodimerization in supercritical CO₂, only the excited singlet state mechanism (eq 12) is considered.

For a quantitative analysis of the anthracene photodimerization results in supercritical CO₂, eq 12 may be simplified. Since the highest anthracene concentration under consideration is only 2.5×10^{-4} M, $k_{DM}[A] \ll 1/\tau_F$

even when k_{DM} is at the diffusion-controlled limit. Under such conditions, eq 12 becomes

$$\Phi_{DIM} = \tau_F k_{DM} [A] \Phi_{A_2} \quad (13)$$

Thus, the intercept of the plot in Figure 5 should be negligible. By forcing the linear regression through the origin, the plot in Figure 5 yields a slope of $1/\tau_F k_{DM} \Phi_{A_2} = 0.034 \text{ M}$. With the fluorescence lifetime τ_F of 7.31 ns at the CO₂ reduced density of 1.9, $k_{DM} \Phi_{A_2} = 4 \times 10^9 \text{ M}^{-1} \text{ s}^{-1}$. For anthracene in normal liquid solvents, k_{DM} is reported to be close to diffusion-controlled. Similarly, k_{DM} in CO₂ may be estimated in terms of the Debye equation:

$$k_{diff} = 8000RT/0.3\eta \quad (14)$$

where η is the shear viscosity of the fluid. At the diffusion-controlled limit, $k_{DM} = k_{diff} = 7 \times 10^{10} \text{ M}^{-1} \text{ s}^{-1}$ in supercritical CO₂ at 35 °C and the reduced density of 1.9. As a result, Φ_{A_2} is calculated to be 0.06, which is smaller than the values reported for anthracene in normal liquid solvents. This is partially due to an overestimation of the diffusion rate constant of anthracene in supercritical CO₂ in terms of the Debye equation. Similar overestimation has been observed for other systems in supercritical fluids.³⁷

The photodimerization of anthracene in supercritical CO₂ is density dependent. At a constant anthracene concentration of $2.5 \times 10^{-5} \text{ M}$, the observed photodimerization yields gradually increase with decreases in CO₂ reduced density. The yield at the reduced density of 1.0 is higher than that at the reduced density of 1.9 by a factor of more than 2. The higher photodimerization yields at lower CO₂ densities may be attributed to more efficient diffusions as a result of lower viscosities. By assuming $k_{DM} = f k_{diff}$, where f is a factor that accounts for the overestimation of diffusion rate constants k_{diff} in CO₂ by the Debye equation, eq 13 becomes

$$\Phi_{DIM} = f \tau_F k_{diff} [A] \Phi_{A_2} \quad (15)$$

By further assuming that f and Φ_{A_2} are CO₂ density independent, Φ_{DIM} may be normalized as follows:

$$\Phi_{DIM}/\Phi_{DIM,\rho_r=1.9} = (\tau_F/\tau_{F,\rho_r=1.9})(\eta/\eta_{\rho_r=1.9}) \quad (16)$$

The $\Phi_{DIM}/\Phi_{DIM,\rho_r=1.9}$ values calculated from eq 16 are compared with the experimentally observed values ($\Phi_{DIM}/\Phi_{DIM,\rho_r=1.9}$)_{OBS} at different CO₂ reduced densities. As shown in Figure 6, there is a reasonable agreement between the experimental and calculated yields. It seems to indicate that the photodimerization of anthracene in

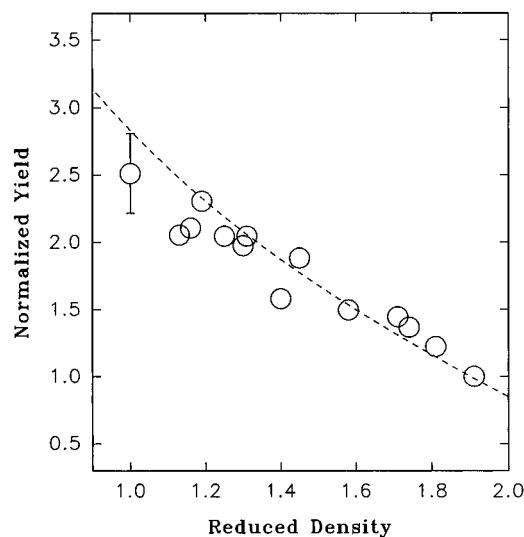


Figure 6. Photodimerization yields of anthracene in supercritical CO₂ at 35 °C as a function of CO₂ reduced density compared with the values calculated from viscosities in terms of the Debye equation. All results are normalized against those at the reduced density of 1.9.

supercritical CO₂ at low fluid densities is also close to diffusion-controlled. The results also suggest that the photodimerization reaction of anthracene is not subject to solute–solvent effects, which are typically more significant in the near-critical density region of a supercritical fluid.^{6,16,17} In the explanation of the large solute–solvent clustering effects on the photofries rearrangement of naphthyl acetate in supercritical CO₂, Weedon and co-workers pointed out the fact that the reaction occurs from the excited singlet state through a very short-lived intermediate and attributed the absence of solute–solvent effects on other reactions to their slower rates with respect to the lifetime of supercritical fluid clusters.⁶ However, the photodimerization of anthracene in supercritical CO₂ is also very fast. The absence of any meaningful solute–solvent clustering effects on the anthracene dimerization reaction indicates that the rate of reactions may not be the only factor in this regard. Further investigations on the mechanism of solute–solvent clustering effects on chemical reactions in supercritical fluids are required.

Acknowledgment. Financial support from the Donors of the Petroleum Research Fund, administered by the American Chemical Society, and in part from the National Science Foundation (CHE-9320558) is gratefully acknowledged. C.E.B. thanks AFOSR for support through the Summer Graduate Research Program.

JO970889A

(37) (a) Sun, Y.-P.; Bunker, C. E. *J. Phys. Chem.* **1995**, *99*, 13778.
 (b) Bunker, C. E.; Sun, Y.-P. *J. Am. Chem. Soc.* **1995**, *117*, 10865.